Indian Geotechnical Journal, 39(2), April 2009, 188 - 200

Effect of Orientation of Micofabric on Engineering Behaviour of Clays

A. Sengupta[1] and L.R. Mantri[2]

Introduction

In soil mechanics, considerable effort has been devoted to the determination of engineering properties of the soil such as shear strength, compressibility, permeability, etc. It is evident that all such properties depend, among other things, upon the geometric arrangement of particles in a soil mass (Anandarajah and Kuganenthira, 1995; Anandarajah et al., 1996; Prashant and Penumadu, 2007; Sachan and Penumadu, 2007). Hence, a study of the geometric arrangement of particles and contact forces between them is needed to understand the behaviour of the soil at micro as well as macro levels. The geometric arrangement of particles in clays can be described in the form of random orientation and preferred orientation. Random orientation refers to clay particles of a sample that are oriented in all possible directions with equal probability, whereas preferred orientation refers to particles that are aligned parallel to each other.

The structure of soils is composed of fabric and inter-particle force system that is governed by soil composition, history, present state, and environment. The influence of soil structure on the engineering behaviour has been recognized from the early stages of soil mechanics, and many researchers have attempted to explain the various aspects of the engineering properties of clays on the basis of its structure. The geometric arrangement of particles, particle groups, and pore spaces is usually defined as the "microfabric" of clays; the existing inter particle force system is referred to as the "stability" of the fabric; and, the term "structure" is used to define the combined effect of clay microfabric and its stability. The concept of fabric has been used to explain the anisotropy and its influence on the observed mechanical behaviour of natural clays.

In the present work, evolution and propagation of shear deformations and pore water pressures in a commercial kaolinite soil with random and preferred orientations of particles are studied under undrained plane strain condition. The experimentally observed responses are also simulated by a finite element program PLAXIS.

---

1 Associate Professor, Dept. of Civil Engg, IIT, Kharagpur 721302; Ph: 03222-283454; Email: sengupta@civil.iitkgp.ernet.in

2 Graduate Student, Dept. of Civil Engg, IIT, Kharagpur 721302.

Experimental Investigations

Test Material and its Properties

In this study a commercially available kaolinite is used as test material. Kaolinite clay has been chosen for this study because of the following reasons:

- It is a stable clay mineral consisting of only one silica and one alumina sheet firmly bonded to each other.
- It is widely distributed in nature and usually the dominant clay mineral because of its relative resistance to chemical weathering.
- It does not swell or expand in the presence of water. Thus the variation in the geometric arrangement of particles could be observed only due to the shear deformation of soil specimens without being influenced by other features.

The commercial kaolinite comes as a homogenous powder, where as natural clay usually will not be homogenous.

The specific gravity of kaolinite used is 2.63. The average values of liquid limit (LL), plastic limit (PL) and plasticity index (PI) are 50.0%, 22.9%, and 27.1%, respectively. As per IS: 1498-1970, the kaolinite may be classified as CI. The average grain size distribution curve of kaolinite is shown in Figure 1. The chemical formula of the kaolinite is $Al_2Si_2O_5(OH)_4$.

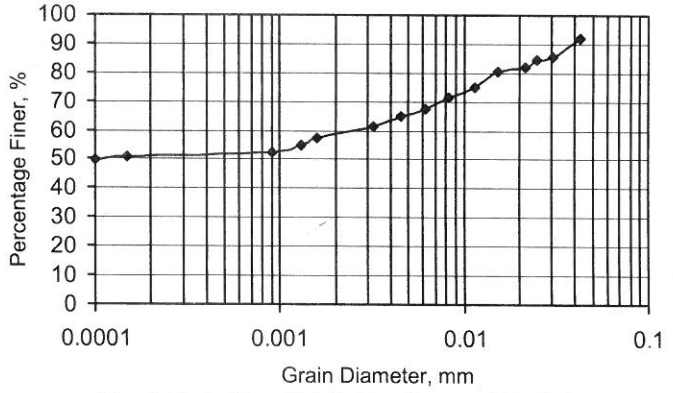

Fig. 1 Grain Size Distribution Curve of Kaolinite.

Preparation of Samples

The commercial kaolinite comes in a powder form, like cement, in 30kg bags. A cylindrical tank is used for the preparation of kaolinite slurry. The 40mm diameter cylindrical slurry tank has both ends open. One end is placed vertically in a sand bath (Figure 2) to facilitate drainage of water through the bottom.

The present investigation is carried on two types of microfabric structures i.e. on flocculated microfabric and dispersed microfabric. The orientations of

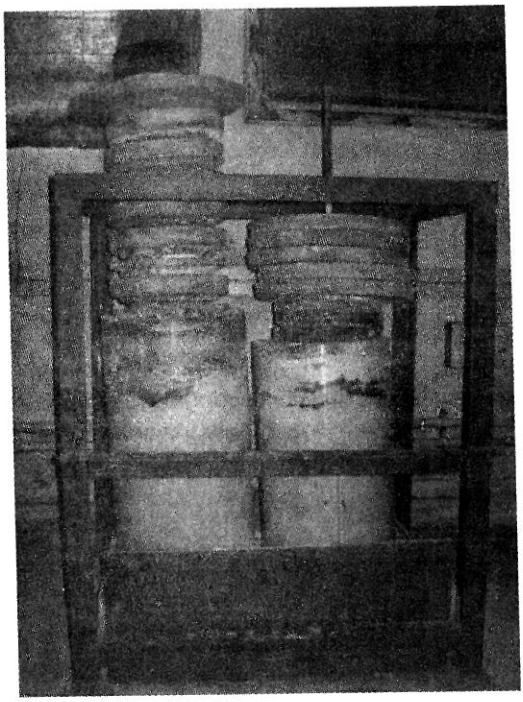

Fig. 2 Slurry Tank

microfabric in both the cases are shown schematically in Figure 3. Specimens with flocculated microfabric (face-to-edge particle contact) are obtained by mixing powered kaolinite with deaired and deionized water at a water content of 150%, and then consolidating the slurry under 275kPa vertical stresses in a cylindrical slurry tank. The dispersed microfabric (face-to-face particle contact) specimens are obtained by using the same procedure and by adding 2% dispersant (calgon) in the clay slurry of 150% water content.

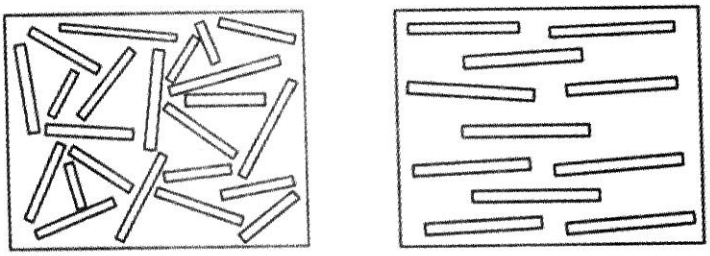

Fig. 3 Microfabric (Schematic) Considered for Kaolinite: (a) Flocculated Microfabric and (b) Dispersed Microfabric

The clay specimens with flocculated microfabric are obtained after 20 to 25 days of consolidation. The dispersed specimens are obtained consolidating the

corresponding slurry for 35 to 40 days. This variation in consolidation time is due to the differences in pore size distribution. The permeability of dispersed specimen along the vertical direction is much smaller than that of the flocculated specimen for identical stress state.

After slurry consolidation, solid rectangular specimens of kaolin clay, each of dimension 70mm width, 140mm height and 25mm thick, with two extreme microfabrics- dispersed and flocculated are extracted with the help of a rectangular split mould of dimensions 150mm x 75mm x 30mm. A thin wire is used to trim the samples, where required, into the desired size. Square grids of 10mm x 10mm in size are imprinted on the samples to monitor the progressive deformations during the tests. An oil-based paint is used to make the grids. The specimen is then inserted into a transparent latex membrane to avoid loss of water during the plane strain test.

Test Procedure

The laboratory plane strain test cell consists of two Perspex plates of 226mm x 146mm x 25mm in size bolted together with the soil specimen sandwiched between them. The bottom end platen is fixed to the two Perspex plates by bolts and is restrained from movement. The top end platen is attached to the assembly in such a way that it can slide smoothly in the vertical direction only, between two fixed guides. All the tests are carried out in undrained condition. The general view of biaxial testing cell is shown in Figure 4.

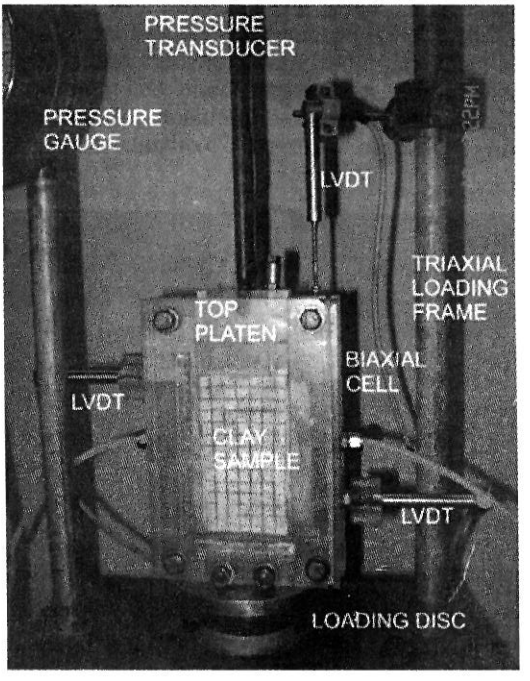

Fig. 4 Biaxial Test Setup

The whole plane strain test device, with soil specimen in it, is mounted on a strain controlled loading frame. The adopted test configuration generates very little friction between the surfaces of the sample and the walls of the Perspex plates. The soil sample is compressed by lowering the top platen at a constant strain rate of 0.125mm per minute. All the experiments and subsequent analysis are done considering effective stresses. Two measuring rulers one in horizontal and another in vertical directions are fixed to the setup to accurately trace the coordinates of the deformed mesh at different stages of the experiments. A stationary digital camera is utilized to record the deformations of the grids with the progress of the tests. The axial load is measured with the help of a load cell. Three linear variable differential transducers (LVDT) are used, for measuring the vertical and the horizontal deformations (Figure 4), respectively. The average pore pressure in the sample is measured with the help of a pressure transducer. A fully computerized data acquisition and control system is utilized to acquire and store all the data with axial loading during the test.

Test Results

The results of plane strain tests done on flocculated and dispersed microfabric kaolinitic clay specimens at zero confining pressure are presented below in terms of deformations at the end of 15% axial strain and in terms of pore pressure versus axial strain and stress versus strain.

Figure 5 shows the evolution of strain localization in both the cases at zero confining pressure. In all the tests, it is observed that shear bands initiate before the peak-stress is reached. In all tests, it initiates around 6 to 7% strain. Around 9-10% axial strain, a single band becomes prominent and emerges from one of the corner. At 12% axial strain, a conjugate band emerges from the other corner. Around 15% axial strain the shear band formation are complete and stresses and pore pressure values drop down to threshold residual values.

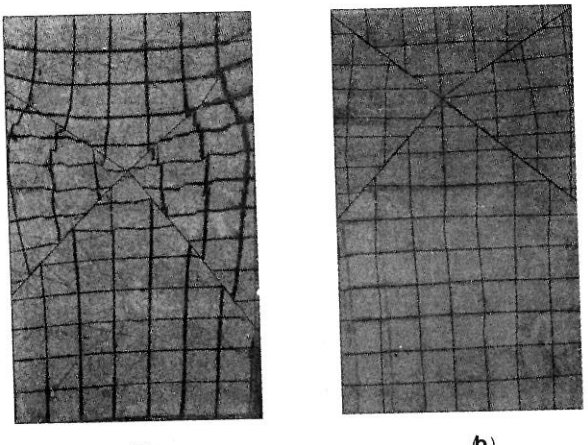

Fig. 5 Deformations of Kaolinite at 15% Strain for (a) Flocculated Microfabric and (b) Dispersed Microfabric

Figures 6 and 7 show the stress and pore pressure with respect to axial strain for tests performed on flocculated and dispersed microfabric kaolinitic clay specimen at zero confining pressure. For the flocculated kaolinitic specimen, the stresses and pore water pressure peak at 8.5% and 7% axial strain, respectively and then drop down sharply. The residual stress at 15% strain is about 46.23kPa. For the kaolinitic specimen with dispersed micofabric, the stresses and pore pressure both peak at 7% axial strain and then after start to drop down sharply. The residual stress at 15% strain is about 64.1kPa.

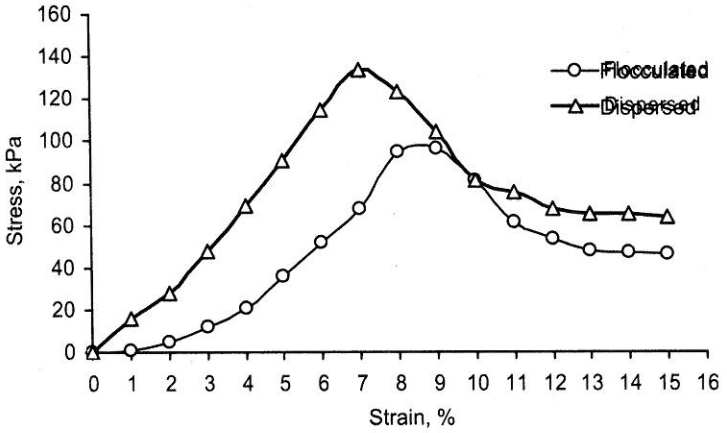

Fig. 6 Stress vs. Strain for both Microfabrics

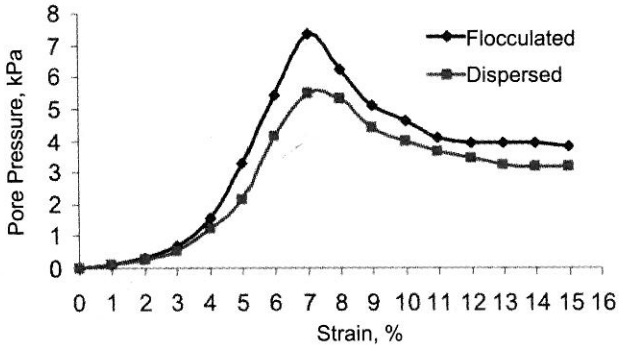

Fig. 7 Pore Pressure vs. Strain for both Microfabrics

From the above figure, it is observed that during the undrained biaxial compression tests on the specimens with dispersed microfabric, positive excess pore-pressure is developed. However, it is significantly lower than the pore-pressure observed in the specimens with flocculated microfabric indicating the less contractive nature of dispersed microfabric. It is also observed that during the undrained biaxial test, dispersed microfabric develop higher shear strength in comparison to flocculated microfabric, and also show well-defined peaks in the stress-strain curves. In dispersed microfabric, the parallel stacking of clay platelets

has the ability to carry a larger amount of axial load applied in a direction perpendicular to the faces of platelets; however, at the same time, these platelets tend to slip suddenly at high stress levels, which leads toa looser configuration of platelets in a local zone induced by the dilative nature of dispersed clay specimens, resulting in peak followed by strain softening responses.

Numerical Analyses

PLAXIS Version 8 (Brinkgreve, 2002) is a finite element package intended for the two – dimensional analysis of deformation and stability in geotechnical engineering. The program allows use of advanced constitutive models for the simulation of the non-linear, time-dependent and anisotropic behaviour of soils and/or rock. In addition, since soil is a multi-phase material, special procedure are available to deal with hydrostatic and non-hydrostatic pore pressures in the soil. PLAXIS is well equipped with features to deal with various aspects of complex geotechnical structures.

The Mohr-Coulomb Model

This robust and simple non-linear model is based on soil parameters that are well-known in engineering practice. The Mohr-Coulomb yield condition is an extension of Coulomb's friction law to general states of stress. In fact, this condition ensures that Coulomb's friction law is obtained in any plane within a material element. The full Mohr-Coulomb yield condition consists of six yield functions when formulated in terms of principal stresses as follows:

$$f_{1a} = \frac{1}{2}(\sigma'_2 - \sigma'_3) + \frac{1}{2}(\sigma'_2 + \sigma'_3)\sin\phi - c\cos\phi \le 0 \quad (1)$$

$$f_{1b} = \frac{1}{2}(\sigma'_3 - \sigma'_2) + \frac{1}{2}(\sigma'_3 + \sigma'_2)\sin\phi - c\cos\phi \le 0 \quad (2)$$

$$f_{2a} = \frac{1}{2}(\sigma'_3 - \sigma'_1) + \frac{1}{2}(\sigma'_3 + \sigma'_1)\sin\phi - c\cos\phi \le 0 \quad (3)$$

$$f_{2b} = \frac{1}{2}(\sigma'_1 - \sigma'_3) + \frac{1}{2}(\sigma'_1 + \sigma'_3)\sin\phi - c\cos\phi \le 0 \quad (4)$$

$$f_{3a} = \frac{1}{2}(\sigma'_1 - \sigma'_2) + \frac{1}{2}(\sigma'_1 + \sigma'_2)\sin\phi - c\cos\phi \le 0 \quad (5)$$

$$f_{3b} = \frac{1}{2}(\sigma'_2 - \sigma'_1) + \frac{1}{2}(\sigma'_2 + \sigma'_1)\sin\phi - c\cos\phi \le 0 \quad (6)$$

where,

σ'_1 = major principal stress (effective)

σ'_2 = intermediate principal stress (effective)

σ'_3 = minor principal stress (effective)

The two plastic model parameters appearing in the yield functions are the well-known friction angle ϕ and the cohesion c. These yield functions together represent a hexagonal cone in principal stress space.

The Basic Parameters for the Mohr-Coulomb Model

The Mohr-Coulomb model requires a total of six parameters, which are obtained from the biaxial test results for both flocculated and dispersed microfabrics. These parameters are bulk density (γ), Young's modulus (E), Poisson's ratio (υ), friction angle (ϕ), cohesion (c) and dilatancy angle (ψ). The value of υ is taken as 0.49 for the undrained condition. Other parameters are given in Table 1.

Table 1 Mohr-Coulomb Parameters for Kaolinite

Fabric Type	E (kPa)	γ (kN/m^3)	ϕ (^{o})	c (kPa)	ψ (^{o})
Flocculated	1896.368	18.75	0	96.0	0
Dispersed	3228.338	19.78	0	134.0	0

The analysis is done by discretizing the sample geometry (70mm wide and 140mm height) with rectangular isoparametric elements and applying the proper boundary conditions. The bottom of the sample is fixed and the top and sides of the clay sample are free. A uniform displacement is applied on the top at uniform rate. All the laboratory tests are simulated in the same manner. For each case, deformations and pore water pressure variations are plotted with the progress of the applied axial strain.

Results of the Numerical Analyses

Figure 8 shows the deformations of flocculated kaolinite specimen at the end of the test (at 15% axial strain).

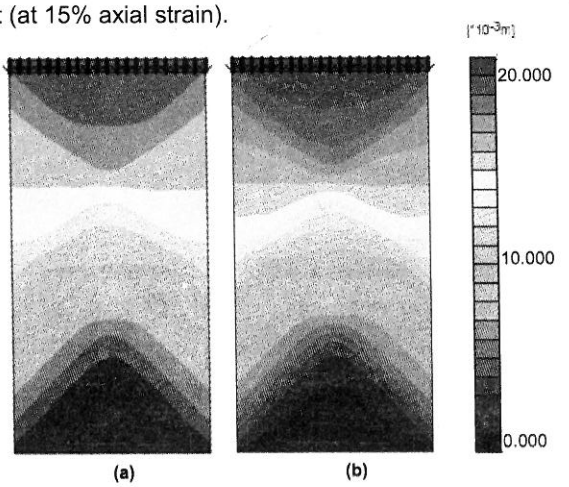

Fig. 8 Deformation at 15% strain in Kaolinite with (a) Flocculated Microfabric; and (b) Dispersed Microfabric

No significant difference in the deformation is found between the kaolinite with flocculated and dispersed microfabrics. However, the numerical model has been found to be capable of capturing strain localization in both the cases.

In the numerical analyses, the pore pressures are estimated at several locations within the samples as shown in Figure 9.

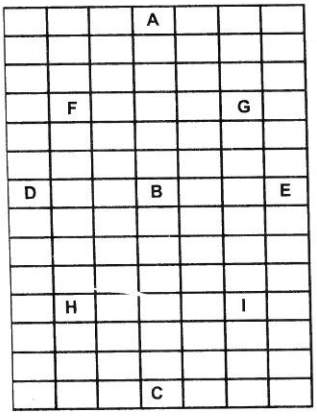

Fig. 9 Locations of Pore Pressures Estimations

Figure 10 shows the pore pressure buildup at various locations in the flocculated microfabric kaolinitic clay matrix.

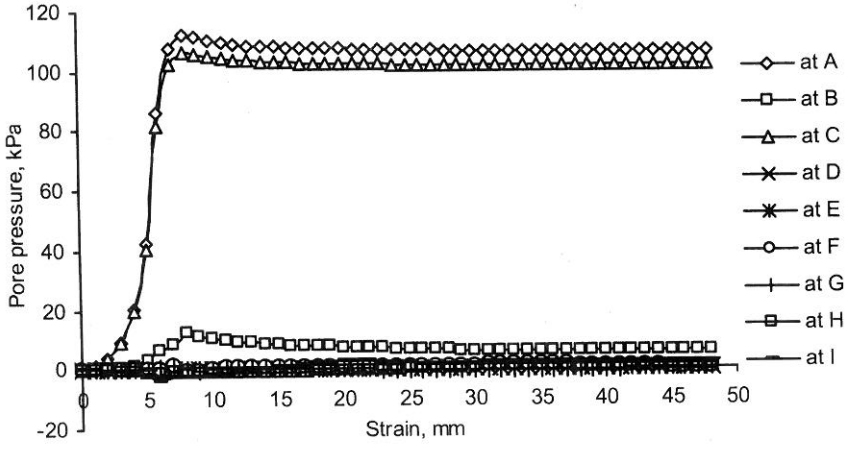

Fig. 10 Pore Pressures in Kaolinite with Flocculated Microfabric

It may be seen from the above figure that the pore pressures are higher near the top and bottom of the kaolinitic sample. The pore pressures drop to zero or negative along the shear bands indicating that the cracks are opening up at these locations causing the pore pressures to drop.

Figure 11 shows the pore pressure buildup at various locations in the dispersed microfabric kaolinitic clay matrix.

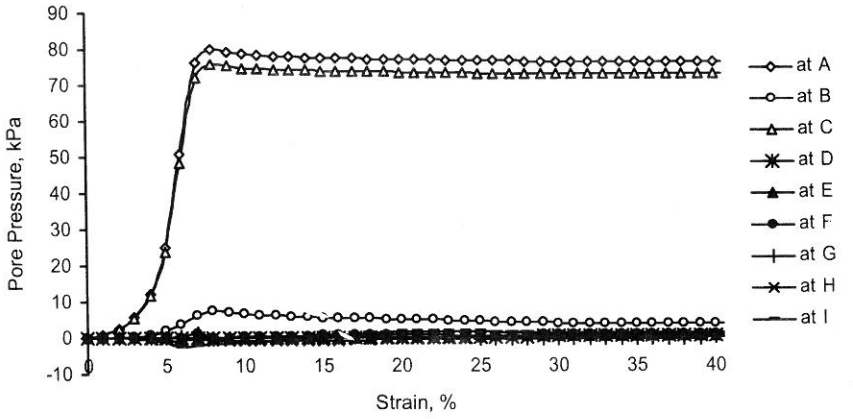

Fig. 11 Pore Pressures in Kaolinite with Dispersed Microfabric

Here also, the pore pressures are higher near the top and bottom of the kaolinitic sample. The pore pressures drop to zero or negative along the shear bands indicating that the cracks are opening up at these locations causing the pore pressures to drop. However, the pore pressures in general are lower in magnitude in the dispersed microfabric compared to the flocculated microfabric. Figures 12 and 13 show the comparison between the average pore pressures obtained in the laboratory experiments and those predicted by the numerical models for both flocculated and dispersed microfabrics.

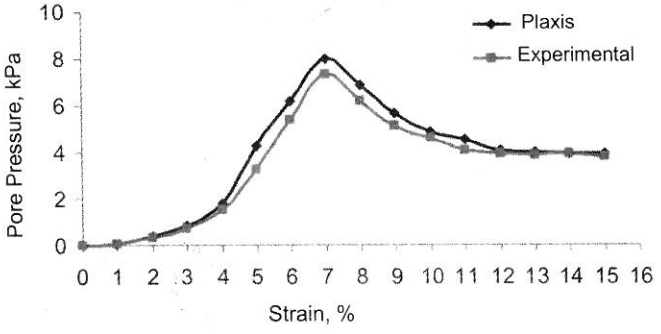

Fig. 12 Comparison of Average Pore Pressures Obtained Experimentally and Predicted Numerically for Kaolinite with Flocculated Microfabric

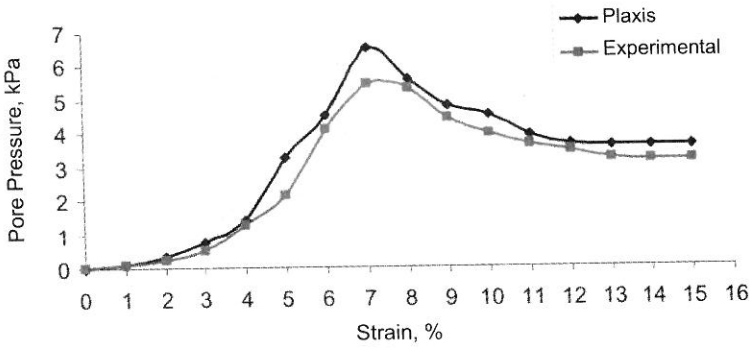

Fig 13 Comparison of Average Pore Pressures Obtained Experimentally and Predicted Numerically for Kaolonite with Dispersed Microfabric

The figures 12 and 13 show that the average pore pressures predicted by the numerical models are reasonably close to the measured average pore pressures in the laboratory tests on kaolinitic clay samples with flocculated and dispersed microfabrics. Both the experimental and the numerical results show that the pore pressures developed in the flocculated microfabric are greater in magnitudes than those in the dispersed microfabric.

Table 2 summarizes the peak and residual pore pressures obtained from the laboratory tests and predicted by the numerical models.

Table 2 Comparison of Pore Pressures

Fabric Type	Peak Pore Pressure (kPa)		Residual Pore Pressure (kPa)	
	Experiment	PLAXIS	Experiment	PLAXIS
Flocculated	7.35	7.98	3.79	3.95
Dispersed	5.47	6.54	3.15	3.58

Conclusions

The current study presents the variation in mechanical behavior of kaolinite clay due to its two extreme microfabrics: dispersed and flocculated. The stress-strain relationships, pore-pressure and shear band evolution for both the microfabrics are investigated both experimentally and numerically. The key observations from this study are summarized as follows:

- It has been found that the shear bands initiated before the peak stress is reached. In all tests, the initiation of the bands is visible at 6-7% axial strain for both the cases.
- In all laboratory tests, ultimately two conjugate shear bands developed at higher axial strains (14-15%) for both the cases.
- The formation of shear bands in an initially homogeneous kaolinite is successfully captured in the laboratory biaxial experiments. The setting of

anisotropy with the progress of the tests is successfully demonstrated in all the tests.

- It is observed that during the undrained biaxial compression tests on the specimens with dispersed microfabric, positive excess pore-pressures are developed. However, it is significantly lower than the pore-pressure evolution observed in the specimens with flocculated microfabric indicating the less contracting nature of dispersed microfabric.
- The undrained biaxial test on dispersed microfabric indicates higher shear strength compared to flocculated microfabric. It also shows well-defined peaks in the stress-strain curves. In dispersed microfabric, the parallel stacking of clay platelets has the ability of carrying a larger amount of axial load applied in a direction perpendicular to the faces of platelets; however, at the same time, these platelets tend to slip suddenly at high stress levels, which leads to a looser configuration of platelets in certain zones induced by the dilative nature of dispersed clay specimens, resulting in peaks followed by strain softening response.
- Stress-strain behaviour of the samples is elastic up to a certain level of strain and then the stress dropped sharply exhibiting a strain softening behaviour with the development of strain localization.
- On increasing the strain further, the stress value levelled off to a residual value considerably less than the peak stress value.
- Before the localization initiates, pore pressure shows a monotonous rise in each test. As the non-uniform deformation sets in, there is a steady downfall in the slope of the pore pressure curve and finally it flattens out to a threshold value at the end.
- Once the shear bands initiate, portion of the soil specimen unload elastically and the rest deforms plastically. Along the shear bands very fine cracks develop and rearrangement of soil particles takes place. Because of this, a decrease in pore pressure is observed during localization of strains. Finally, when the shear bands develop fully and a stable condition is obtained, the pore pressure levels out at a threshold value.
- The finite element package PLAXIS is successfully utilized to measure pore-pressure buildup and deformation of kaolinite soil samples with flocculated and dispersed microfabrics.
- The pore pressures along the shear bands are much lesser than the pore pressures developed outside (top & bottom) the shear band. This is because of the formation of fine cracks along the shear bands.
- The results obtained from PLAXIS are in good agreement with those obtained from the laboratory experiments.

References

Anadarajah, A., Kuganenthira, N. and Zhao, D. (1996): 'Variation of Fabric Anisotropy of Kaolinite in Triaxial Loading', *Journal of Geotechnical Engineering*, ASCE, 122(8), pp. 633-640.

Anadarajah, A. and Kuganenthira, N. (1995): 'Some Aspects of Fabric Anisotropy of Soil', *Geotechnique*, 45(1), pp. 69-81.

Brinkgreve, R. B. J. (2002): *PLAXIS (2D)-Version 8, Manual*, Delft University of Technology and PLAXIS b.v., The Netherlands.

Prashant, A. and Penumadu, D. (2007): 'Effect of Microfabric on Mechanical Behavior of Kaolin Clay Using Cubical True Triaxial Testing', *Journal of Geotechnical and Geoenvironmental Engineering*, ASCE, 133(4), pp. 433-444.

Sachan, A. and Penumadu, D. (2007): 'Effect of Microfabric on Shear Behaviour of Kaolin Clay', *Journal of Geotechnical and Geoenvironmental Engineering*, ASCE, 133(3), pp. 306-318.